Stark Effect in Wild-Type and Heterodimer-Containing Reaction Centers from *Rhodobacter capsulatus*†

Theodore J. DiMagno,‡,§ Edward J. Bylina,‖,⊥ Alexander Angerhofer,‡,# Douglas C. Youvan,‖ and James R. Norris*,‡,§

Chemistry Division, Argonne National Laboratory, Argonne, Illinois 60439, Department of Chemistry, University of Chicago, Chicago, Illinois 60615, and Department of Chemistry, Massachusetts Institute of Technology, Cambridge, Massachusetts 02139

Received May 19, 1989; Revised Manuscript Received August 30, 1989

ABSTRACT: The effect of an external electric field on the optical absorption spectra of wild-type *Rhodobacter capsulatus* and two *Rb. capsulatus* reaction centers that have been genetically modified through site-directed mutagenesis ($His^{M200} \rightarrow Leu^{M200}$ and $His^{M200} \rightarrow Phe^{M200}$) was measured at 77 K. The two genetically modified reaction centers replace histidine M200, the axial ligand to the M-side bacteriochlorophyll of the special pair, with either leucine or phenylalanine. These substitutions result in the replacement of the M-side bacteriochlorophyll with bacteriopheophytin, forming a bacteriochlorophyll–bacteriopheophytin heterodimer. The magnitude of the change in dipole moment from the ground to excited state ($\Delta\mu_{app}$) and the angle δ between the Q_y transition moment and the direction of $\Delta\mu_{app}$ were measured for the special pair absorption band for all three reaction centers. The values for $\Delta\mu_{app}$ and δ obtained for wild-type *Rb. capsulatus* ($\Delta\mu_{app} = 6.7 \pm 1.0$ D, $\delta = 38 \pm 3°$) were the same within experimental error as those of *Rhodobacter sphaeroides* and *Rhodopseudomonas viridis*. The values for $\Delta\mu_{app}$ and δ obtained for the red-most Stark band of both heterodimers were the same, but $\Delta\mu$ was substantially different from that of wild-type reaction centers ($His^{M200} \rightarrow Leu^{M200}$, $\Delta\mu_{app} \geq 14.1$ D and $\delta = 33 \pm 3°$; $His^{M200} \rightarrow Phe^{M200}$, $\Delta\mu_{app} \geq 15.7$ D and $\delta = 31 \pm 4°$). The differences in the magnitude of $\Delta\mu_{app}$ and the angle δ between wild-type and heterodimer reaction centers are consistent with increased charge transfer in the heterodimer special pair. These results support calculations that place the special pair charge-transfer state higher in energy than the excited singlet state in wild-type *Rb. capsulatus* RCs.

Photosynthesis is the process that converts incident light energy into electrochemical potential energy through a series of ultrafast electron transfer reactions in the photosynthetic reaction centers (RCs).[1] The X-ray crystal structure of two photosynthetic bacterial RCs, *Rhodopseudomonas viridis* and *Rhodobacter sphaeroides*, has recently been determined (Deisenhofer et al., 1984; Chang et al., 1986; Allen et al., 1987). This structure confirmed that the primary donor in these RCs consists of a dimeric bacteriochlorophyll special pair (Norris et al., 1971). The charge separation process is initiated by the absorption of light by the special pair to form the excited singlet state, designated *P. A charge-transfer state within the excited singlet state of the special pair was proposed to explain the primary electron transfer in photosynthesis (Norris & Katz, 1978). This primary electron transfer occurs to form the initial radical pair species P^+BPh^- in less than 3.5 ps, and the electron is then transferred from there to the quinone of the iron–quinone complex in 200 ps (Kirmaier & Holten, 1987). The mechanism of the second, slower electron transfer reaction rate is as expected from conventional electron transfer theory (Marcus & Sutin, 1985). However, the mechanism of the ultrafast first electron transfer reaction requires more consideration. Even though many recent theoretical (Creighton et al., 1988; Marcus, 1987; Scherer & Fischer, 1987; Plato et al., 1988) and experimental (deLeeuv et al., 1982; Boxer et al., 1986; Popovic et al., 1985) works have addressed this problem, the nature of the excited singlet state of the primary donor needs further elucidation if a theoretical model for the ultrafast electron transfer reaction is to be established.

One method of probing the first excited state is by applying a large external electric field to the RCs and monitoring the changes in the photosynthetic process. Considerable work on electrochromic effects in the general area of photosynthesis started about 20 years ago (Kleuser & Bücher, 1969; Emrich et al., 1969). More recently, electrochromism (Stark effect spectroscopy) has been used to study the singlet excited state of the BChl special pair dimer. deLeeuv et al. (1982) reported a large Stark effect in the Q_y absorption of the photosynthetic bacteria *Rb. sphaeroides*. The value of the Stark effect in the dimer band was first quantitated by Lockhart et al. (1987) and later confirmed by Lösche et al. (1987). Both groups suggested that the large Stark effect may be due to a mixing of the charge-transfer state ($BChl^+$–$BChl^-$) with the excited singlet state (*P) of the bacteriochlorophyll dimer.

One method to examine this hypothesis is to alter the constitutents of the special pair, the moiety that is responsible

† This work was supported by the U.S. Department of Energy, Office of Basic Energy Sciences, Division of Chemical Sciences, under Contract W-31-109-Eng-38. A.A. acknowledges support by the Deutsche Forschungsgemeinschaft Grant AN/160-1.

‡ Argonne National Laboratory.

§ University of Chicago.

‖ Massachusetts Institute of Technology.

⊥ Current address: Biotechnology Program, Pacific Biomedical Research Center, University of Hawaii at Manoa, Honolulu, HI 96822.

On leave from The University of Stuttgart, Stuttgart, West Germany.

[1] Abbreviations: BChl, bacteriochlorophyll; BPh, bacteriopheophytin; CT, charge transfer; D, primary electron donor special pair bacteriochlorophyll–bacteriopheophytin heterodimer in genetically modified reaction centers; EPR, electron paramagnetic resonance; P, primary electron donor special pair bacteriochlorophylls in wild-type reaction centers; PVA, poly(vinyl alcohol); RCs, reaction centers.

0006-2960/90/0429-899$02.50/0

for the excited singlet state. Reaction centers from *Rb. capsulatus* have been genetically modified through site-directed mutagenesis (Bylina & Youvan, 1987). Two of these genetically modified RCs replace histidine M200, the axial ligand to the M-side BChl of the special pair, with either leucine or phenylalanine (Bylina & Youvan, 1988). These substitutions result in the replacement of the M-side BChl with BPh, forming a BChl–BPh heterodimer. The pigment content of the heterodimer RCs was confirmed by pigment extractions. The $His^{M200} \rightarrow$ Leu RCs gave a total pigment content of 5.7 ± 0.1 and a BChl/BPh ratio of 1.0 ± 0.1, and for $His^{M200} \rightarrow$ Phe RCs the total pigment content was 5.8 ± 0.2 with a BChl/BPh ratio of 1.1 ± 0.1. The heterodimer RCs also differ from wild type in quantum yield and rate of electron transfer. The quantum yield of the electron transfer from D to $D^+BPh_L^-$ is 55% in $His^{M200} \rightarrow$ Leu RCs, much lower than the 100% yield for wild type. The time constant for this electron transfer reaction is 31 ps, much slower than the 3.5-ps time constant for wild type (Kirmaier et al., 1988). These dramatic differences in the electron transfer process make the heterodimer an excellent choice for studying the excited singlet state. In this work we have measured the Stark spectra of wild-type and two heterodimer-containing RCs from *Rb. capsulatus*. The differences and similarities in the Stark spectrum of these three RCs are discussed. These results may shed light on the nature of the first excited singlet state.

Materials and Methods

Wild-type, $His^{M200} \rightarrow$ Leu, and $His^{M200} \rightarrow$ Phe reaction centers of *Rb. capsulatus* were isolated by described procedures (Bylina & Youvan, 1988; Prince & Youvan, 1987). RC films were prepared by adding RCs to a 10% poly(vinyl alcohol) (PVA) solution. The films were cast and dried for 2 days at 277 K under a nitrogen atmosphere to yield typical films ranging from 50 to 120 μm in thickness. The Stark cell consisted of a RC/PVA film between two copper wire mesh electrodes (200 wires/in., 78% transmission, Buckbee-Mears Co.) mounted between two glass plates. The high-voltage leads were attached to the mesh electrodes with Teflon screw clamps. For angular dependence studies of ΔA, the Stark cell was mounted on a goniometer and rotated such that the polarized light vector made an angle θ with the electric field vector (Mathies & Stryer, 1976). The sample was submerged directly into liquid nitrogen in an optical Dewar, and the probing beam made a single pass through the sample and the semitransparent mesh electrodes. The Stark spectrometer is the same as described previously (Lockhart & Boxer, 1987; Lösche et al., 1987), and we calibrated our spectrometer with *Rb. sphaeroides* RCs and obtained qualitative and quantitative agreement with their results.

We checked the quality of our film preparations by making films under reducing (ascorbic acid sodium salt and sodium dithionite) and oxidizing (potassium ferrocyanide) conditions. We found that the Stark spectra were qualitatively unchanged for films prepared under reducing conditions but the two red-most Stark bands were absent from the spectra for films prepared under oxidizing conditions (data not shown). We also improved our goniometer to reduce errors in our angle dependence studies and obtained a more precise value for δ in the heterodimers than we previously reported (Norris et al., 1989). The values presented here are in better agreement with recent results on similar *Rb. sphaeroides* heterodimers (S. Boxer, personal communication).

The absorption spectrum of the RC/PVA films was taken at 77 K in a commerical spectrometer equipped with a liquid N_2 Dewar, and the base line of the absorption spectrum was corrected for scattered light to yield a flat base line. The abscissa of the spectrum was then converted to wavenumbers in the computer. The weighted second-derivative term $\nu\, d^2(A/\nu)/d\nu^2$ was obtained from the second derivative of the absorption curve in wavenumbers with $\Delta\nu$ = 7.7–31.7 cm^{-1}, and then the second derivative was multiplied by the wavenumber in the computer.

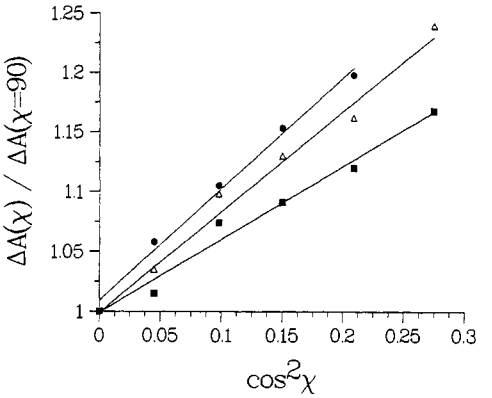

FIGURE 1: From the slope of the line found from the plot of $\Delta A(\chi)/\Delta A(\chi{=}90°)$ vs $\cos^2\chi$, the angle δ was determined from eq 2 for RCs from wild-type *Rb. capsulatus* (■), *Rb. capsulatus* $His^{M200} \rightarrow$ Phe (●), and *Rb. capsulatus* $His^{M200} \rightarrow$ Leu (△). The straight lines are the least-squares fit of the plotted data points. Each data point represents the average of three to ten individual data points. This plot clearly shows that the two heterodimer RCs have approximately the same angle δ, but they both differ slightly from the angle δ found for wild-type RCs.

The angular dependence measurements were analyzed similarly to the method used by Lösche et al. (1987) to determine the angle δ between the transition moment vector μ_{trans} and the change in dipole moment vector $\Delta\mu_{app}$. The incident light was polarized perpendicular to the sample rotation axis. χ was determined from the geometric relationship in eq 1, where

$$\chi = \frac{\pi}{2} - \sin^{-1}\left(\frac{n_{liq\,N_2}}{n_{PVA}}\sin\phi\right) \qquad (1)$$

the angle of incidence is ϕ, $n_{liq\,N_2}$ is the refractive index of liquid nitrogen, and n_{PVA} is the refractive index of PVA. From a plot of $\Delta A(\chi)/\Delta A(\chi{=}90°)$ vs $\cos^2\chi$ (Figure 1), the angle δ can be obtained from eq 2, where s is the slope of the line in

$$\delta = \cos^{-1}\left(\frac{2s+1}{s+2}\right)^{1/2} \qquad (2)$$

Figure 1. The Stark effect, ΔA, was determined from the Taylor series expansion of ΔA for small absorption changes, $\Delta A = \Delta I_{rms}/(I_0 \ln 10)$. The difference in the excited-state and ground-state dipole moments $\Delta\mu$ is obtained from $\Delta\mu = \Delta\mu_{app}/f$, where F_{rms} is the external electric field, f is the local field correction, and $\Delta\mu_{app}$ is given by eq 3.

$$\Delta\mu_{app} = \frac{hc}{F_{rms}}\left[\frac{10\sqrt{2}\Delta A}{(1+\sin^2\delta)\dfrac{\nu\, d^2(A/\nu)}{d\nu^2}}\right]^{1/2} \qquad (3)$$

Results

The absorption, second-derivative, and Stark spectra at 77 K for the Q_x and Q_y absorption bands of wild-type, $His^{M200} \rightarrow$ Leu, and $His^{M200} \rightarrow$ Phe reaction centers from *Rb. capsulatus* are shown in Figures 2–7. The Q_y Stark spectra for wild-type *Rb. capsulatus* (Figure 2) show the same features as those for *Rb. sphaeroides* R-26 (Lockhart & Boxer, 1988)

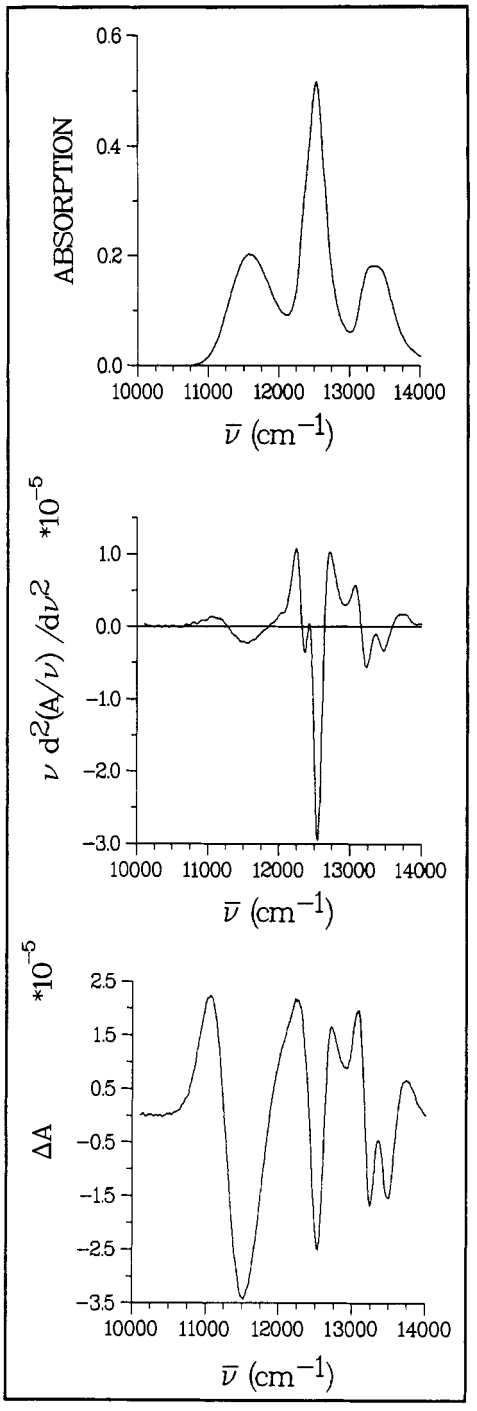

FIGURE 2: Absorption (top), weighted second-derivative (middle), and Stark spectrum (bottom) for the Q_y region of wild-type *Rb. capsulatus* reaction centers embedded in PVA films at 77 K. The absorption spectrum was taken on a commercial spectrometer, and base-line correction was applied. The second derivative was calculated in the computer from the absorption spectrum. The stark spectrum was taken with a single scan with an applied external electric field, F_{ext} = 283 kV/cm.

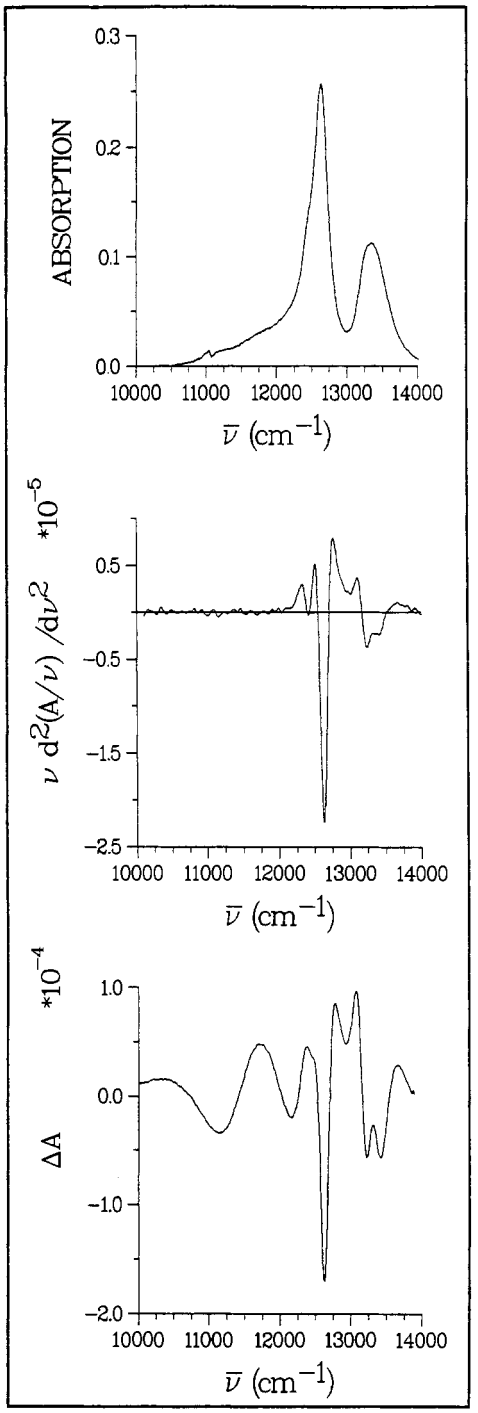

FIGURE 3: Absorption (top), weighted second-derivative (middle), and Stark spectrum (bottom) for the Q_y region of *Rb. capsulatus* His^{M200} → Phe reaction centers embedded in PVA films at 77 K. The absorption spectrum was taken on a commercial spectrometer, and base-line correction was applied. The second derivative was calculated in the computer from the absorption spectrum. The Stark spectrum was taken with a single scan with an applied external electric field, F_{ext} = 375 kV/cm.

and *Rp. viridis* (Lösche et al., 1987; Braun et al., 1987). The four resolved Stark bands in the Q_y absorption region consist of the two partially resolved components of the bacteriopheophytin absorption band at 13 515 and 13 263 cm^{-1}, the 12 549-cm^{-1} accessory bacteriochlorophyll, and the large Stark band at 11 530 cm^{-1} corresponding to the special pair bacteriochlorophylls. The decrease in resolution (only four resolved Stark bands in wild-type *Rb. capsulatus* compared to five resolved Stark bands for *Rb. sphaeroides* R-26) can be easily explained by the smaller red shift of the special pair absorption band in wild-type *Rb. capsulatus*. The large Stark band at 11530 cm^{-1} in *Rb. capsulatus* overlaps and obscures the small band which can be resolved in *Rb. sphaeroides*.

The absorption, second-derivative, and Stark spectra for His^{M200} → Phe (Figure 3) and His^{M200} → Leu RCs (Figure 4) are nearly identical with each other. Not only are the heterodimer Stark spectra similar to each other, but they also mimic many features of the wild-type Stark spectra. The heterodimer RCs have similar resolved Stark bands (at 13 425, 13 234, and 12 634 cm^{-1} for His^{M200} → Phe RCs and at 13 425,

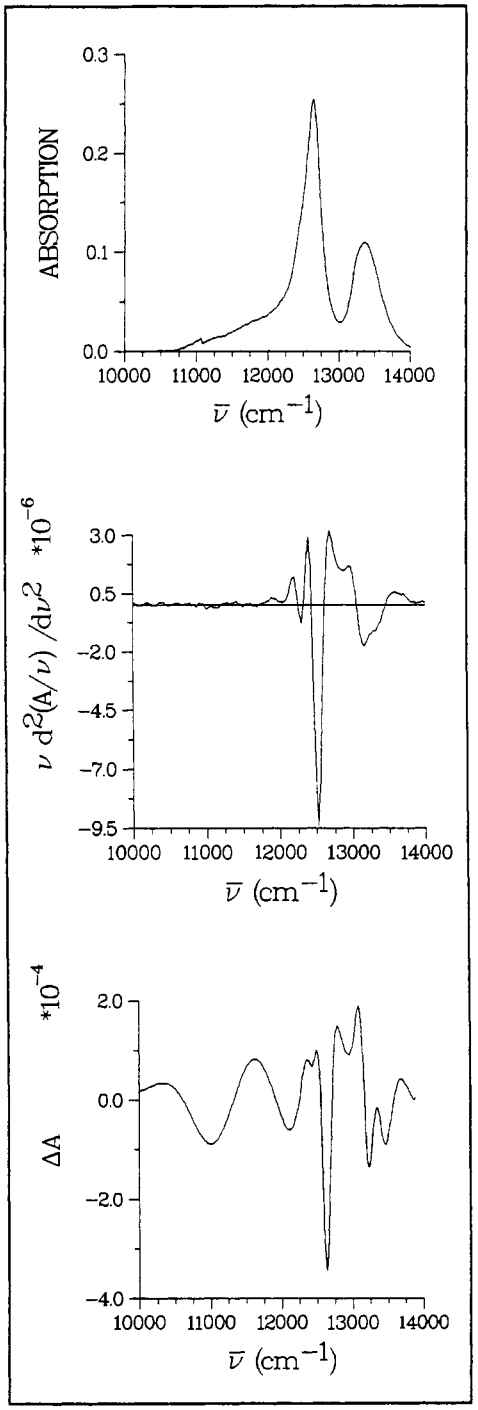

FIGURE 4: Absorption (top), weighted second-derivative (middle), and Stark spectrum (bottom) for the Q_y region of *Rb. capsulatus* His^{M200} → Leu reaction centers embedded in PVA films at 77 K. The absorption spectrum was taken on a commercial spectrometer, and base-line correction was applied. The second derivative was calculated in the computer from the absorption spectrum. The Stark spectrum was taken with a single scan with an applied external electric field, F_{ext} = 250 kV/cm.

13 240, and 12 639 cm^{-1} for His^{M200} → Leu RCs), with each band having a similar shape and relative magnitude as those of wild type. These similarities suggest that the His^{M200} → Leu and His^{M200} → Phe substitutions did not result in large structural changes throughout the RCs. In addition to these three resolved Stark bands, the His^{M200} → Leu RC has a fully resolved band at 12 474 cm^{-1}, and the His^{M200} → Phe RC has a partially resolved band at 12 431 cm^{-1}. These bands are similar to the second component of the band resolved at 12 240 cm^{-1} in *Rb. sphaeroides* (Lösche et al., 1987), but this band

Table I: Comparison of the Direction and Magnitude of the Apparent Dipole Moments, $\Delta\mu_{app}$, in Photosynthetic Bacteria[a]

photosynthetic bacteria	δ (deg)	$\Delta\mu_{app}$ (D)	simulated $\Delta\mu_{app}$ (D)
Rb. sphaeroides R-26	38 ± 3	6.6 ± 1.0	6.0
Rb. capsulatus wild-type	38 ± 3	6.7 ± 1.0	6.3
Rb. capsulatus His^{M200} → Leu	33 ± 3	≥14.1	43.0
Rb. capsulatus His^{M200} → Phe	31 ± 4	≥15.7	41.0

[a] The direction, δ, and magnitude of the cahnge in dipole moment, $\Delta\mu_{app}$, calculated from the Stark spectra taken at 77 K. Also included is the value of $\Delta\mu_{app}$ calculated from the simulation of the absorption spectrum with a sum of Gaussians located at the minimum of the Stark bands. The local field correction can be included in the calculation to obtain the change in dipole moment, $\Delta\mu$, between the ground and excited states with the equation $\Delta\mu = f^{-1}\Delta\mu_{app}$, where f accounts for the local field correction. We have left out a discussion on the local field correction because it is dependent on the assumptions you make about the local field, and it does not change any feature of the Stark spectrum except the absolute magnitude of the dipole moment change. See Lockhart and Boxer (1987) and Lösche et al. (1987) for a further discussion of the local field approximation, where the calculated change in dipole moment decreases by a factor of 1.2–1.7 depending on which local field model was used and which parameter was used for the protein dielectric constant. [The results for *Rb. sphaeroides* in this table are from DiMagno and Norris (unpublished results)].

is not resolved in wild-type *Rb. capsulatus*. There are also two other resolved Stark bands which are substantially different in the genetically modified RCs. These two broad bands are at 12 110 and 11 020 cm^{-1} for the His^{M200} → Leu RCs and at 12 162 and 11 147 cm^{-1} for the His^{M200} → Phe RCs. Neither of these Stark bands has a corresponding absorption band that can be clearly distinguished in the broad tail of the absorption spectrum. Even though these Stark bands have no corresponding Stark band in wild-type *Rb. capsulatus*, the band around 12 150 cm^{-1} for both species resembles the small negative signal at ~11 500 cm^{-1} in *Rp. viridis* (Lockhart & Boxer, 1988) between the special pair and accessory bacteriochlorophyll band.

Before the quantitative analyses of $\Delta\mu_{app}$ and δ were determined, the optical density change, ΔA, was measured as a function of the magnitude of the applied electric field. According to theory, ΔA should vary quadratically with the changing electric field since $\Delta A \propto (F_{rms})^2$ (see eq 3). For all three *Rb. capsulatus* RCs studied in this work, the electric field was varied up to a factor of 2.7 (163–438 kV/cm). The corresponding change in ΔA for all three RCs was within 3% of an exact quadratic dependence (data not shown). Moreover, the line shape of all bands in the Stark spectrum is independent of the 2.7-fold increase in applied electric fields.

The angle δ and the value $\Delta\mu_{app}$ were calculated for the red-most Stark band for the three *Rb. capsulatus* RCs (and also for *Rb. sphaeroides* R-26 RCs for comparison) and are listed in Table I. The angle δ was determined from eq 2, and $\Delta\mu_{app}$ was determined from eq 3 with the experimentally measured values ΔA, F_{rms}, δ, and $\nu\, d^2(A/\nu)/d\nu^2$. The results for the wild-type *Rb. capsulatus* 11 530-cm^{-1} band at 77 K (δ = 38°, $\Delta\mu_{app}$ = 6.7 D) are the same as those for both *Rb. sphaeroides* and *Rp. viridis* (Lösche et al., 1987; Lockhart & Boxer, 1988) RCs within experimental error. Both His^{M200} → Leu and His^{M200} → Phe RCs have the same value of δ and $\Delta\mu_{app}$ at 77 K (His^{M200} → Leu, δ = 33° and $\Delta\mu_{app} \geq$ 14.1 D; His^{M200} → Phe, δ = 31° and $\Delta\mu_{app} \geq$ 15.7 D), but the value for $\Delta\mu_{app}$ differs substantially from that of wild-type *Rb. capsulatus* RCs.

The Stark spectra for the Q_x absorption region are shown in Figures 5–7. The signal to noise ratio is lower due to the smaller Stark effect in the Q_x region (an order of magnitude smaller intensity than the Q_y region). Due to the complex

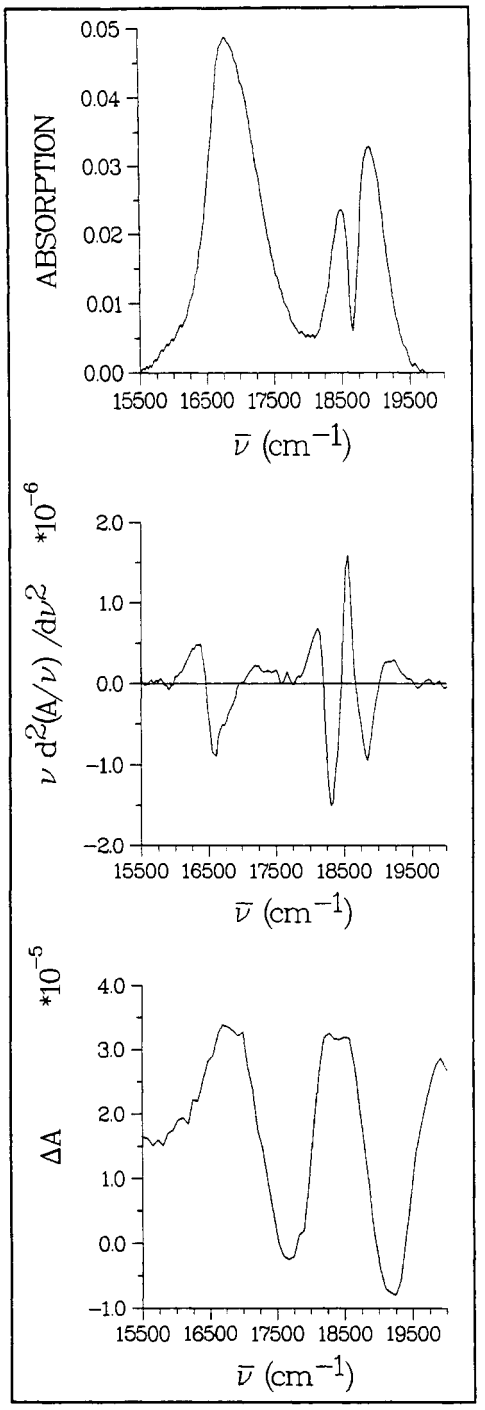

FIGURE 5: Absorption (top), weighted second-derivative (middle), and Stark spectrum (bottom) for the Q_x region of wild-type *Rb. capsulatus* reaction centers embedded in PVA films at 77 K. The absorption spectrum was taken on a commercial spectrometer, and base-line correction was applied. The second derivative was calculated in the computer from the absorption spectrum. The Stark spectrum was taken with a single scan with an applied external electric field, F_{ext} = 283 kV/cm.

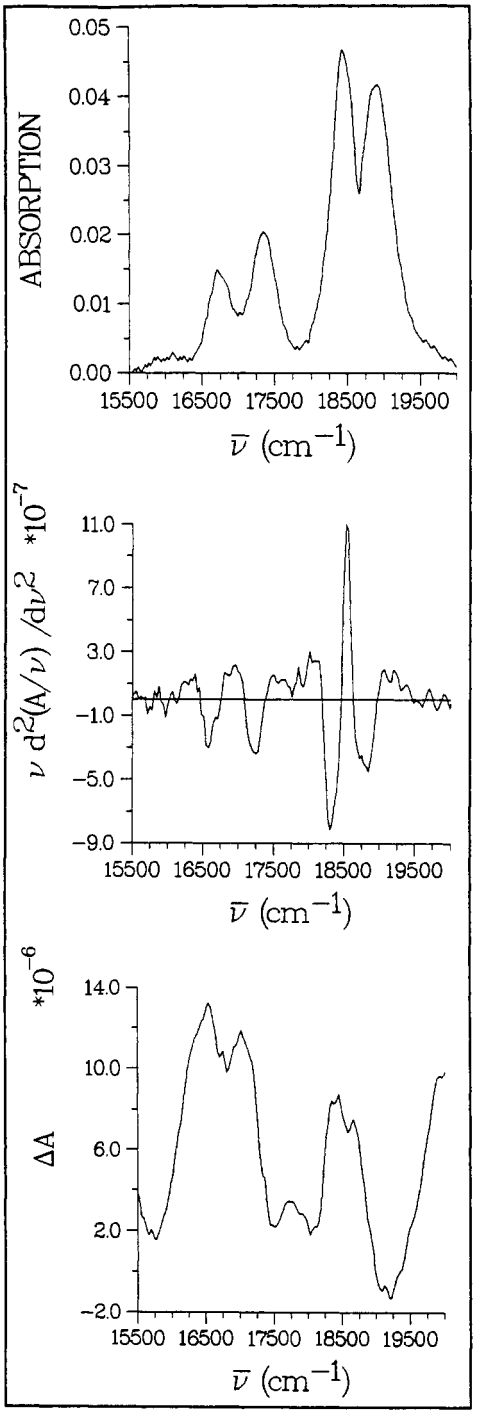

FIGURE 6: Absorption (top), weighted second-derivative (middle), and Stark spectrum (bottom) for the Q_x region of *Rb. capsulatus* His^{M200} → Phe reaction centers embedded in PVA films at 77 K. The absorption spectrum was taken on a commercial spectrometer, and base-line correction was applied. The second derivative was calculated in the computer from the absorption spectrum. The Stark spectrum was taken with a single scan with an applied external electric field, F_{ext} = 375 kV/cm.

shape of the Q_x Stark spectra, both the positive and negative bands are reported. Figure 5 shows two resolved negative bands at 17 700 and 19 200 cm^{-1} and two positive bands at 16 700 and 18 400 cm^{-1} for wild-type reaction centers. Notice that these bands vary dramatically from the second-derivative line shape and have a substantial contribution from the first-derivative line shape. This may be due to a breakdown in the approximation that the change in polarizability $\Delta\alpha$ is small compared to the change in the dipole moment $\Delta\mu$. This would make the inclusion of the term linear in $\Delta\alpha$ ($\Delta A \approx [\Delta\alpha F^2\, d(A/\nu)/d\nu]/2hc$) necessary (Liptay, 1974), thus adding a first-derivative term to the shape of the Q_x Stark spectra.

The Stark spectrum for the His^{M200} → Phe RCs Q_x region is shown in Figure 6 and is very similar to the wild-type spectrum, except that more bands are resolved in the His^{M200} → Phe spectrum due to the new peak in the Q_x absorption spectra. The negative band at 17 600 cm^{-1} in wild-type RCs is resolved into two bands at 17 400 and 18 100 cm^{-1} in His^{M200} → Phe RCs. The two other negative bands are at 19 100 and 15 750 cm^{-1}. The red-most positive band is also split into two

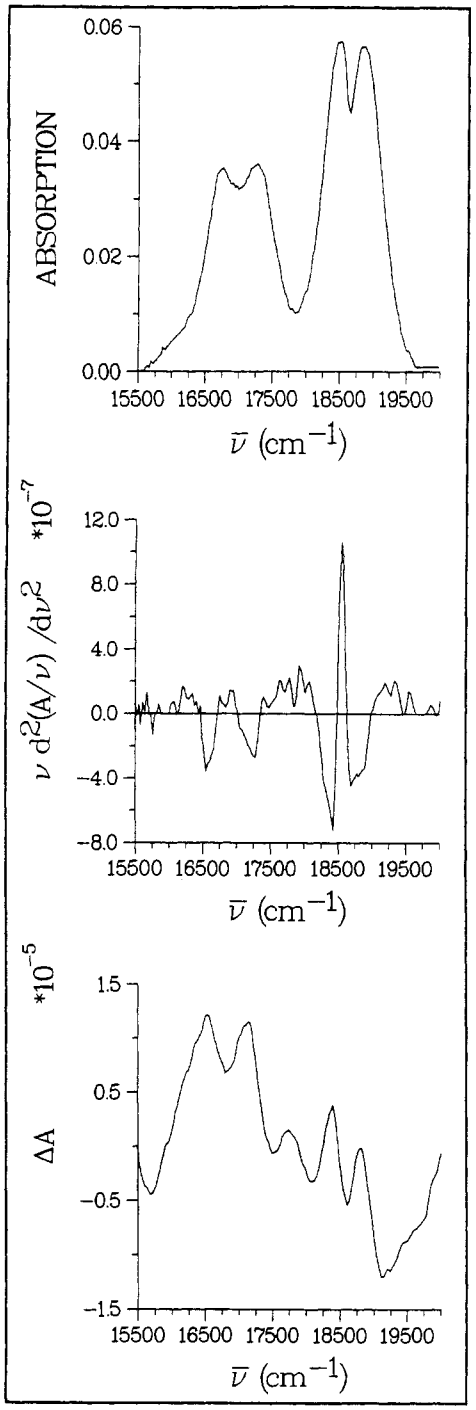

FIGURE 7: Absorption (top), weighted second-derivative (middle), and Stark spectrum (bottom) for the Q_x region of *Rb. capsulatus* His^{M200} → Leu reaction centers embedded in PVA films at 77 K. The absorption spectrum was taken on a commercial spectrometer, and base-line correction was applied. The second derivative was calculated in the computer from the absorption spectrum. The Stark spectrum was taken with a single scan with an applied external electric field, F_{ext} = 250 kV/cm.

bands at 16 400 and 17 000 cm^{-1}, and the other positive band is split into two bands at 18 400 and 18 700 cm^{-1}.

The Stark spectrum for the His^{M200} → Leu RCs is shown in Figure 7 and is nearly identical with that of the His^{M200} → Phe RCs except for the further resolution of the blue-most positive peak. The increased resolution and decreased amplitude of the central positive peak nearly obscure the two positive peaks at 18 400 and 18 800 cm^{-1}. The red-most positive band is split into two peaks at 16 500 and 17 000 cm^{-1}. The four negative Stark bands are at 19 200 and 15 750 cm^{-1} with the split central band at 18 000 and 17 500 cm^{-1}.

Discussion

The nature of the excited state, *P (or *D for the heterodimer RCs), can be examined by Stark spectroscopy using *Rb. capsulatus* RCs. The magnitude of $\Delta\mu_{app}$ for His^{M200} → Leu and His^{M200} → Phe RCs is larger than that for wild-type RCs for the red-most band. If the state responsible for the large Stark effect within the special pair is charge transfer (CT) in character, then this suggests that even more charge transfer is present in the heterodimers. The ultrafast evolution of the charge-transfer state is also suggested by transient absorption difference spectroscopy (Kirmaier et al., 1988). Some calculations estimate that the relative energy of the charge-transfer state is above that in the exciton state in wild-type RCs (Parson & Warshel, 1987). When the constituents of the charge-transfer state change from $BChl_L^+BChl_M^-$ → $BChl_L^+BPh_M^-$ in the heterodimer, the energy of this state will decrease by ~0.3 eV (Fajer et al., 1975), and this should narrow the energy gap between the exciton and CT states. This decrease in energy of the charge-transfer state should cause the corresponding heterodimer CT Stark band to red shift relative to that of wild-type RCs. A Stark band is observed for both His^{M200} → Leu and His^{M200} → Phe RCs that is red-shifted ~500 cm^{-1} from the special pair Stark band in wild-type *Rb. capsulatus* RCs. This suggests that this Stark band is from a CT state, thus supporting the idea that there is more charge-transfer character present within the first excited singlet state of the primary donor in the heterodimer RCs. This conclusion is also consistent with the investigation by Kirmaier et al. (1988), who speculated that the state *D in the heterodimer may be the pure intradimer charge-transfer state ($BChl_L^+BPh_M^-$) to explain the time-resolved transient absorption difference spectra and the decreased rate of electron transfer (31 ps) to the initial radical pair state.

Highly coupled to any conclusions in this work is the interpretation of the ordinary optical absorption spectrum of the heterodimer RCs, most importantly that no distinct red-shifted optical band characteristic of the special pair is evident in the broad absorption tail. Four main factors can contribute to the weakness and breadth of the absorption shoulder in the heterodimers. (i) The exciton state is lifetime broadened due to the ultrafast formation of a charge-transfer state (Kirmaier et al., 1988), thus causing the absorption to be homogeneously broadened. (ii) The oscillator strength of the Q_y absorption should be ~25% smaller due to the decrease in oscillator strength of bacteriopheophytin relative to the bacteriochlorophyll that it replaces in the special pair (van der Rest & Gingras, 1974). (iii) The structure could be a "loose" distribution of configurations, thus causing the absorption band to be inhomogeneously broadened. (iv) The presence of a nearby CT state is expected to broaden the absorption spectrum (Won & Friesner, 1988). We feel that the inhomogeneously broadened absorption line shape is not consistent with the two well-defined Stark bands in this absorption region. This leaves us with lifetime broadening of the exciton state (not the charge-transfer state, which seems to be stable for ~14 ps in the heterodimer RCs), a decrease in oscillator strength, and the presence of a CT state to explain the loss of a well-resolved Q_y absorption band for the heterodimers in the His^{M200} → Leu and His^{M200} → Phe RCs.

The values for $\Delta\mu_{app}$ listed in Table I were calculated with eq 3. The largest error in determining this value was in determining the value for the weighted second derivative, because of the poor signal to noise ratio due to the broad nature of the special pair absorption band. In the case of the two hetero-

dimer RCs, no second-derivative signal could be detected for the red-most Stark bands. From the magnitude of the noise in this spectrum, we could place limits on the size of the weighted second derivative. The maximum magnitude of the weighted second derivative is -2.4×10^{-7} for $His^{M200} \rightarrow Phe$ RCs and -1.7×10^{-7} for $His^{M200} \rightarrow Leu$ RCs. These values correspond to minima for $\Delta\mu_{app}$ of 15.7 for $His^{M200} \rightarrow Phe$ and 14.1 for $His^{M200} \rightarrow Leu$ RCs. Since we were unable to obtain exact values for $\Delta\mu_{app}$, the value for $\Delta\mu_{app}$ was calculated by an alternative approximation method. The absorption spectra were fitted by a sum of Gaussian curves located at the center of each observed Stark band. Five Gaussians were used for wild-type RCs, and six Gaussians were used for $His^{M200} \rightarrow$ Phe and $His^{M200} \rightarrow$ Leu RCs. The weighted second derivative was determined from the fitted spectra by the same procedure as described previously. From this simulation method, the weighted second derivative for wild type was -1.5×10^{-6}, resulting in a value of $\Delta\mu_{app} = 6.3$ D, an error of only 6% from the experimental result. For the $His^{M200} \rightarrow$ Phe and $His_{M200} \rightarrow$ Leu RCs, the value of the weighted second derivative for the fitted absorption spectra was -6.7×10^{-9}, yielding a value of $\Delta\mu_{app}$ 2.6 times larger than the minimum experimental value for $His^{M200} \rightarrow$ Phe and 3.0 times larger than the minimum experimental value for $His^{M200} \rightarrow$ Leu. This value ($\sim$40 D) approximates the dipole moment expected for a full point charge separated by 7.6 Å. This raises the possibility that the observed Stark band is due to a full charge-transfer state as speculated by Kirmaier et al. (1988). Even though these results seem to be in agreement, we cannot conclusively confirm that a full charge-transfer state exists. Since the simulation was performed with a simplified Gaussian model, we can only use these results as a limiting case. From the experimental and simulation data, we are only able to bracket the value for $\Delta\mu_{app}$ for the heterodimers between 14 and 43 D. Even though the value for $\Delta\mu_{app}$ is larger in the heterodimer, this does not necessarily correspond to an increase in the amount of charge-transfer character. In wild-type RCs, C_2 symmetry would require a linear combination of the two possible special pair charge-transfer states ($BChl_L^+BChl_M^-$ and $BChl_L^-BChl_M^+$). The value of $\Delta\mu_{app}$ could be due to the predominance of one of these two states because of the asymmetry of the protein environment. However, the increase in the asymmetry of the heterodimer charge-transfer state ($BChl_L^+BPh_M^-$) could cause an increase in $\Delta\mu_{app}$ without increasing the total amount of charge-transfer character associated with the primary donor, because the heterodimer CT state is not an average of two states.

The problems in determining and analyzing $\Delta\mu_{app}$ in the heterodimer RCs cannot be completed with the current data. Future experiments that improve the signal to noise ratio for the determination of the weighted second derivative will hopefully resolve the discrepancy between the experimental and simulation values. While this uncertainty in the weighted second derivative affects the value of $\Delta\mu_{app}$, it should not affect the value of δ, the angle between the transition moment and the change in dipole moment vectors.

Both the Stark data and the transient absorption data suggest a rather asymmetric heterodimer special pair. Because of the difference in redox potentials between bacteriochlorophyll and bacteriopheophytin, the sharing of spin density should be unequal in the oxidized heterodimer. This result is confirmed (Bylina et al., unpublished results) in electron paramagnetic resonance (EPR) experiments on the two heterodimers. The EPR line width from wild-type RCs suggested a special pair dimer $^+(BChl_LBChl_M)$ (Norris et al., 1971), while the EPR line width from the heterodimer-containing RCs suggested a monomeric $^+BChl_L$ electron donor. The asymmetric charge distribution of the oxidized heterodimer confirmed the notion that an internal CT state within the heterodimer special pair would be more favored due to the difference in redox potentials of the different heterodimer constituents.

Although no crystal structure exists for *Rb. capsulatus*, linear dichroism shows that the orientations of pigments with respect to the membrane direction in wild-type, $His^{M200} \rightarrow$ Leu, and $His^{M200} \rightarrow$ Phe RCs are similar to each other and to those of RCs in *Rb. sphaeroides* R-26 (Breton et al., 1989). We will relate our Stark data to the crystal structure of *Rp. viridis* RCs, because of the high resolution of this crystal structure. This structure approximates the structure of *Rb. sphaeroides* because the later structure was solved by a molecular replacement of the *Rp. viridis* structure, and it should also approximate the structure of *Rb. capsulatus*.

The angle δ between the transition moment vector and the change in dipole moment vector eventually should be interpreted in terms of the reaction center structure. At present a precise correlation with the molecular structure determined by X-ray diffraction is impossible without accurate electronic wave functions of the special pair and until the directions of both $\Delta\mu$ and Q_y are known precisely. In the absence of such knowledge, the direction of the Q_y transition moment is approximated as the average of the Q_y transition moments of the two bacteriochlorophylls that make up the special pair. Since the special pair exhibits approximate C_2 symmetry, the averaged transition moment also has C_2 symmetry, in agreement with the experimental results on single crystals of *Rp. viridis* (Zinth et al., 1983). Clearly, the assumed C_2 symmetry will be invalid in the heterodimer because of the difference in optical properties of bacteriopheophytin and bacteriochlorophyll; therefore, the transition moment direction of the heterodimer is expected to change relative to that of wild-type RCs. The other aspect of interpreting the angle δ, namely, estimating the direction of $\Delta\mu$, is much more difficult. Consequently, any precise interpretation of the magnitude and the direction of δ in terms of the molecular structure of the reaction center is not yet possible.

In our measurements, we interpret the change in δ between wild-type and heterodimer RCs as due to this effective breaking of the C_2 symmetry, which could be broken in two distinct ways in the heterodimer. One would be the change in the Q_y transition moment direction as just mentioned above. The other would be the change in the direction of $\Delta\mu_{app}$, where the direction of $\Delta\mu_{app}$ can also be changed by altering the charge-transfer nature of the special pair. As have others, we assume that $\Delta\mu_{app}$ arises from the excited state only, since the ground-state dipole moment is thought to be negligible. For a pure charge-transfer state in wild-type RCs that rigorously possess C_2 symmetry, the 2-fold symmetry requires that there be an equal linear combination of the two possible charge-transfer configurations ($^+BChl_L^-BChl_M$) and ($^+BChl_M^-BChl_L$), yielding the two states $\psi_1 = [\alpha(^+BChl_L^-BChl_M) + \alpha(^+BChl_M^-BChl_L)]$ and $\psi_2 = [\beta(^+BChl_L^-BChl_M) - \beta(^+BChl_M^-BChl_L)]$. Previous Stark spectra indicate that in wild-type RCs these two states are mixed unequally. For the heterodimer RCs, the two possible charge-transfer states are expected to mix unequally because the symmetry is severely broken in the donor. Since the CT state ($^+BChl_L^-BPh_M$) is much more stable due to the lower redox potential of BPh compared to BChl, this state is expected to dominate in the heterodimer RCs. To model this effect, the direction of each

individual CT state ($^{+}BCh_L^{-}BChl_M$, $^{+}BChl_M^{-}BChl_L$, and $^{+}BChl_L^{-}BPh_M$) was determined from the spin densities of $^{+}$BChl, $^{-}$BChL, and $^{-}$BPh (Fajer et al., 1977) located at their respective position in the crystal structure. By use of this approach the direction of $\Delta\mu_{app}$ in wild-type RCs is the appropriate average of the two vectors, $^{+}BChl_L^{-}BChl_M$ and $^{+}BChl_M^{-}BChl_L$; in the heterodimer-containing RCs the direction of $\Delta\mu_{app}$ is given by the vector $^{+}BChl_L^{-}BPh_M$. The angle between each charge-transfer state vector and a $\Delta\mu_{app}$ determined for a hypothetical C_2 charge-transfer donor (i.e., equal mixing) is 19.5°. Thus, 19.5° estimates the maximum change in the direction of $\Delta\mu_{app}$ that can be expected and is quite consistent with our results.

Conclusions

In summary, we emphasize several aspects of our Stark data. First, we point out that the correct interpretation of the normal optical spectrum of all three *Rb. capsulatus* RCs is necessary to properly explain their Stark spectrum. The conclusions reached in this paper assume that our interpretation of the broad optical spectra of the heterodimer RCs is correct. Second, the intensity of the optical density changes in $His^{M200} \rightarrow$ Phe and $His^{M200} \rightarrow$ Leu RCs is about the same size as in wild-type *Rb. capsulatus*. This observation seems to rule out the possibility that the lack of structural integrity causes the low intensity of the red band in the normal optical absorption spectrum for the heterodimer RCs. If the lack of structural integrity of the heterodimer special pair were responsible for the weak intensity of the optical spectrum in the red region, a corresponding negligible Stark spectrum would be expected due to the inhomogeneous broadening of the optical band. Third, the intensity of the Stark spectrum changes quadratically with the magnitude of the applied electric field, indicating that the phenomenon we are measuring in the *Rb. capsulatus* RCs is consistent with the theory of electrochromism. Fourth, the same interpretational technique as used by others (Lockhart & Boxer, 1987; Scherer & Fischer, 1986) gives results on the dipole moment change and its relative angle similar to previous studies of charge separation within the special pair for wild-type *Rb. capsulatus* RCs. This interpretation is correct if the Stark bands have only a second-derivative line shape. However, the Stark bands are somewhat asymmetric and may have zero- or first-order contributions mixed in with the second derivatives. The presence of these terms could affect the results concluded in this paper. Fifth, the change in the angle δ and the difference in $\Delta\mu_{app}$ for the heterodimer are consistent with its increased asymmetrical nature. Sixth, the CT state in wild-type RCs is higher in energy than the singlet excited state as previously predicted (Parson & Warshel, 1987).

These results support the view that charge transfer internal to the special pair is especially relevant to the observed Stark effects. However, much more remains to be explained satisfactorily, such as the additional structure in the heterodimer Stark spectra and the well-resolved red-shifted Stark bands relative to the broad tail in the normal optical spectrum. Consequently, a more detailed and quantitative analysis of these results is in progress.

Acknowledgments

We thank Dr. J. Deisenhofer and Dr. H. Michel for making the crystal coordinates of *Rp. viridis* available to us. We also thank Dr. R. Friesner and Dr. S. Boxer for helpful discussions and Dr. Harvey Drucker for support.

References

Allen, J. P., Feher, G., Yeates, T. O., Komiya, H., & Rees, D. C. (1987) *Proc. Natl. Acad. Sci. U.S.A. 84*, 5730–5734.

Boxer, S. G., Middendorf, T. R., & Lockhart, D. J. (1986) *FEBS Lett. 200*, 237–241.

Braun, H. P., Michel-Beyerle, M. E., Breton, J., Buchanan, S., & Michel, H. (1987) *FEBS Lett. 221*, 221–225.

Breton, J., Bylina, E. J., & Youvan, D. C. (1989) *Biochemistry* (in press).

Bylina, E. J., & Youvan, D. C. (1987) *Z. Naturforsch. 42C*, 769–774.

Bylina, E. J., & Youvan, D. C. (1988) *Proc. Natl. Acad. Sci. U.S.A. 85*, 7226–7230.

Bylina, E. J., Kirmaier, C., McDowell, L., Holten, D., & Youvan, D. C. (1988) *Nature 336*, 182–184.

Chang, C.-H., Tiede, D., Tang, J., Smith, U., Norris, J., & Schiffer, M. (1986) *FEBS Lett. 205*, 82–86.

Creighton, S., Hwang, J.-K., Warshel, A., Parson, W. W., & Norris, J. R. (1988) *Biochemistry 27*, 774–781.

Deisenhofer, J., Epp, O., Miki, K., Huber, R., & Michel, H. J. (1984) *J. Mol. Biol. 180*, 385–398.

deLeeuv, D., Malley, M., Buttermann, G., Okamura, M. Y., & Feher, G. (1982) *Biophys. J. 37*, 111a.

Emrich, H. M., Junge, W., & Witt, H. T. (1969) *Z. Naturforsch. 24B*, 1144–1146.

Fajer, J., Brune, D. C., Davis, M. S., Forman, A., & Spaulding, L. D. (1975) *Proc. Natl. Acad. Sci. U.S.A. 72*, 4956–4960.

Fajer, J., Forman, A., Davis, M. S., Spaulding, L. D., Brune, D. C., & Felton, R. H. (1977) *J. Am. Chem. Soc. 99*, 4134–4140.

Kirmaier, C., & Holten, D. (1987) *Photosynth. Res. 13*, 225–260.

Kirmaier, C., Holten, D., Bylina, E. J., & Youvan, D. C. (1988) *Proc. Natl. Acad. Sci. U.S.A. 85*, 7562–7566.

Kleuser, D., & Bücher, H. (1969) *Z. Naturforsch. 24B*, 1371–1374.

Liptay, W. (1974) in *Excited States* (Lim, E. C., Ed.) Vol. 1, pp 129–229, Academic Press, New York.

Lockhart, D. J., & Boxer, S. G. (1987) *Biochemistry 26*, 664–668.

Lockhart, D. J., & Boxer, S. G. (1988) *Proc. Natl. Acad. Sci. U.S.A. 85*, 107–111.

Lösche, M., Feher, G., & Okamura, M. Y. (1987) *Proc. Natl. Acad. Sci. U.S.A. 84*, 7537–7541.

Marcus, R. A. (1987) *Chem. Phys. Lett. 133*, 471–477.

Marcus, R. A., & Sutin, N. (1985) *Biochim. Biophys. Acta 811*, 265–322.

Mathies, R., & Stryer, L. (1976) *Proc. Natl. Acad. Sci. U.S.A. 73*, 2169–2173.

Norris, J. R., & Katz, J. J. (1978) in *The Photosynthetic Bacteria* (Clayton, R. K., & Sistrom, W. R., Eds.) pp 397–418, Plenum Press, New York and London.

Norris, J. R., Uphaus, R. A., Crespi, H. L., & Katz, J. J. (1971) *Proc. Natl. Acad. Sci. U.S.A. 68*, 625–628.

Norris, J. R., DiMagno, T. J., Angerhofer, A., Chang, C.-H., El-Kabbani, O., & Schiffer, M. (1989) in *22nd Jerusalem Symposium on Perspectives in Photosynthesis* (Pullman, P., & Jortner, J., Eds.) D. Reidel Press, Dordrecht and Boston (in press).

Parson, W. W., & Warshel, A. (1987) *J. Am. Chem. Soc. 109*, 6152–6163.

Plato, M., Möbius, K., Michel-Beyerle, M. E., Bixon, M., & Jortner, J. (1988) *J. Am. Chem. Soc. 110*, 7279–7285.

Popovic, Z. D., Kovacs, G. J., Vincett, P. S., & Dutton, P. L. (1985) *Chem. Phys. Lett. 116*, 405–410.

Prince, R. C., & Youvan, D. C. (1987) *Biochim. Biophys. Acta 890*, 286-291.
Scherer, P. O. J., & Fischer, S. F. (1986) *Chem. Phys. Lett. 131*, 153-159.
Scherer, P. O. J., & Fischer, S. F. (1987) *Chem. Phys. Lett. 141*, 179-185.
van der Rest, M., & Gingras, G. (1974) *J. Biol. Chem. 249*, 6446-6453.
Won, Y., & Friesner, R. A. (1988) *J. Phys. Chem. 92*, 2214-2219.
Zinth, W., Kaiser, W., & Michel, H. (1983) *Biochim. Biophys. Acta 723*, 121-131.

Deglycosylation of Chondroitin Sulfate Proteoglycan and Derived Peptides†

S. C. Campbell,‡ R. C. Krueger,§ and N. B. Schwartz*

Department of Pediatrics and Department of Biochemistry and Molecular Biology, University of Chicago, Joseph P. Kennedy, Jr., Mental Retardation Research Center, 5841 South Maryland Avenue, Box 413, Chicago, Illinois 60637

Received April 24, 1989; Revised Manuscript Received August 2, 1989

ABSTRACT: In order to define the domain structure of proteoglycans as well as identify primary amino acid sequences specific for attachment of the various carbohydrate substituents, reliable techniques for deglycosylating proteoglycans are required. In this study, deglycosylation of cartilage chondroitin sulfate proteoglycan (CSPG) with minimal core protein cleavage was accomplished by digestion with chondroitinase ABC and keratanase, followed by treatment with anhydrous HF in pyridine. Nearly complete deglycosylation of secreted proteoglycan was verified within 45 min of HF treatment by loss of incorporated [^{3}H]glucosamine label from the proteoglycan as a function of time of treatment, as well as by direct analysis of carbohydrate content and xylosyltransferase acceptor activity of unlabeled core protein preparations. The deglycosylated CSPG preparations were homogeneous and of high molecular weight (approximately 370 000). Comparison of the intact deglycosylated core protein preparations with newly synthesized unprocessed precursors (apparent M_r ~360 000) suggested that extensive proteolytic cleavage of the core protein did not occur during normal intracellular processing. Furthermore, peptide patterns generated after clostripain digestion of core protein precursor and of deglycosylated secreted proteoglycan were comparable. With the use of the clostripain digestion procedure, peptides were produced from unlabeled proteoglycan, and two predominant peptides from the most highly glycosylated regions (the chondroitin sulfate rich regions of the proteoglycan) were isolated, characterized, and deglycosylated. These peptides were found to follow similar kinetics of deglycosylation and to acquire xylose acceptor activity comparable to the intact core protein.

Chondroitin sulfate proteoglycan (CSPG)[1] consists of a core protein to which various types of carbohydrate chains are attached. Studies using cultured chondrocytes from embryonic chick sterna (Habib et al., 1984; Campbell & Schwartz, 1988) or from the rat chondrosarcoma (Kimura et al., 1981; Fellini et al., 1984) have contributed significantly to our understanding of the events involved in the assembly of proteoglycans. Extensive posttranslational processing of the core protein involves addition of N-linked oligosaccharides and xylose in the RER (Habib et al., 1984; Hoffman et al., 1984), followed by addition of the remainder of the glycosaminoglycan chains and O-linked oligosaccharides (Thonar et al., 1983) and processing of the N-linked oligosaccharides in the Golgi apparatus. All of these steps lead to the formation of a very large and polydisperse proteoglycan [M_r ~(1-4) × 10^6], which is approximately 90% carbohydrate by weight (Hassell et al., 1986). The polydispersity observed in proteoglycans synthesized by cultured rat chondrosarcoma chondrocytes can be primarily accounted for by variations in the number or size of the attached carbohydrate chains (Fellini et al., 1981). However, several studies using proteoglycans synthesized in vivo indicate that heterogeneity in the length of the core protein may also contribute to this polydispersity (Rosenberg et al., 1976; Thyberg et al., 1975; Heinegard, 1977; Buckwalter & Rosenberg, 1982). Newly synthesized core protein, immunoprecipitated from the RER of both rat chondrosarcoma and embryonic chick sternal cultured chondrocytes, has yielded a molecular weight value of 370 000 by SDS-polyacrylamide electrophoresis (Habib et al., 1984; Kimura et al., 1981). Also cell-free translation of mRNA from either system (Vertel et al., 1984) yielded immunospecific core protein which was homogeneous and also of rather large molecular weight (M_r ~340 000). These results can be contrasted with the few available estimates for the size of the core protein in the completed proteoglycan. Chondroitinase and keratanase (when necessary) digestion of proteoglycan from rat chondrosarcoma or chick epiphyses resulted in preparations of core protein which consisted of 60% protein by weight and migrated on SDS-PAGE with an apparent molecular weight of 400 000 (Kimura et al., 1981; Kimata et al., 1982; Oike et al., 1982). This would give an estimate for the molecular weight of the

† This investigation was supported in part by USPHS Grants RO1-AR-19622, HD-17332, and PO1-HD-09402.
* Address correspondence to this author at the Department of Pediatrics, University of Chicago.
‡ Supported by MSTP Grant GM-07281.
§ Supported by MD/PhD Training Grant HD-07009.

[1] Abbreviations: CSPG, chondroitin sulfate proteoglycan; RER, rough endoplasmic reticulum; Endo H, endo-β-*N*-acetylglucosaminidase H; SDS, sodium dodecyl sulfate; PAGE, polyacrylamide gel electrophoresis; PITC, phenyl isothiocyanate; DTT, dithiothreitol; EDTA, ethylenediaminetetraacetate; PMSF, phenylmethanesulfonyl fluoride; NEM, *N*-ethylmaleimide; HBSS, Hank's balanced salt solution; Tris, tris(hydroxymethyl)aminomethane; GuHCl, guanidine hydrochloride.

0006-2960/90/0429-907$02.50/0